Master's Thesis

Virus–nucleus interactions in late herpesvirus infection

Satu Hakanen

University of Jyväskylä

Department of Biological and Environmental Science

Cell and Molecular Biology

16.11.2017

Preface

This Master's Thesis was carried out in the virus-cell interactions research group of Maija Vihinen-Ranta. I wholeheartedly want to thank Dr. Maija Vihinen-Ranta for granting me the opportunity to join this group. As my supervisor, your encouraging attitude and experience on the field made the completion of this thesis a rewarding learning process.

I would also like to express a special gratitude to Dr. Elina Mäntylä, especially for being a skilled instructor in practical laboratory work. Another thank you goes to these important people who kindly offered technical assistance along the way: Petri Papponen, Lassi Palmujoki and Jani Järvensivu.

The electron microscopy data gathered for this thesis have additionally been published in two recent research papers:

Myllys, M., V. Ruokolainen, V. Aho, E.A. Smith, S. Hakanen, P. Peri, A. Salvetti, J. Timonen, V. Hukkanen, C.A. Larabell, and M. Vihinen-Ranta. 2016. Herpes simplex virus 1 induces egress channels through marginalized host chromatin. *Sci.Rep.* 6:28844

Aho, V., M. Myllys, V. Ruokolainen, S. Hakanen, E. Mantyla, J. Virtanen, V. Hukkanen, T. Kuhn, J. Timonen, K. Mattila, C.A. Larabell, and M. Vihinen-Ranta. 2017. Chromatin organization regulates viral egress dynamics. *Sci.Rep.* 7:3692-017-03630-y

University of Jyväskylä
Faculty of Mathematics and Science

Abstract of Master's Thesis

Author: Satu Hakanen
Title of thesis: Virus – nucleus interactions in late herpesvirus infection
Finnish title: Viruksen ja tuman vuorovaikutukset myöhäisessä herpesvirusinfektiossa
Date: 16.11.2017 **Pages:** 42

Department: Department of Biological and Environmental Science
Chair: Cell Biology
Supervisor(s): Maija Vihinen-Ranta

Abstract:

Herpes simplex virus 1 (HSV-1) is an enveloped icosahedral dsDNA virus, and a common human pathogen with an estimated incidence of 67% in the global population. Infected individuals permanently carry the latent HSV-1 in neuronal cells. Sporadic virus reactivation into the lytic life cycle typically manifests as facial lesions known as cold sores. HSV-1 utilizes the host cell nucleus for genome replication and nucleocapsid assembly. Nuclear interior is occupied by viral replication compartments, whereas the host chromatin becomes compressed and marginalized to the nuclear periphery. Progeny nucleocapsids exit the intact nucleus by budding through the nuclear envelope. While the mechanism of nuclear egress has been well-characterized, less is known about progeny nucleocapsid movement among the host chromatin to the inner nuclear membrane. The aim of this study was to observe the properties of host chromatin in relation to viral replication compartments and progeny nucleocapsids during the late phase of lytic HSV-1 infection. In order to gain a more detailed look into the host chromatin as a structural element, we studied the redistribution of the loosely packed active euchromatin and the compacted silent heterochromatin by labeling their respective histone post-translational modifications. Confocal and transmission electron microscopy (TEM) imaging of HSV-1 infected nuclei showed that the marginalized host chromatin forms an uneven ring, which contains gaps that allow progeny nucleocapsids to access the inner nuclear membrane for egress. Nanometer-scale visualization of nucleocapsids in TEM images revealed that nucleocapsids are frequently surrounded by an electron-lucent, halo-like space, which might be related to nucleocapsid movement through the host chromatin. Notably, active euchromatin appears in the nuclear periphery adjacent to the inner nuclear membrane upon infection, although it is yet unclear if this finding represents virally activated euchromatin. Chromatin remodeling is a prominent feature of lytic HSV-1 infection. Further characterization of the key interactions between host chromatin and viral components could expose critical steps in HSV-1 nuclear egress, which might have additional value as therapeutic targets of this widespread human virus.

Keywords: HSV-1, herpesviruses, nucleus, chromatin, virus-nucleus interactions

Jyväskylän yliopisto
Matemaattis-luonnontieteellinen tiedekunta

Pro gradu –tutkielman tiivistelmä

Tekijä: Satu Hakanen
Tutkielman nimi: Viruksen ja tuman vuorovaikutukset myöhäisessä HSV-1-infektiossa
English title: Virus – nucleus interactions in late HSV-1 infection
Päivämäärä: 16.11.2017 **Sivumäärä:** 42

Laitos: Bio- ja ympäristötieteiden laitos
Oppiaine: Solubiologia
Tutkielman ohjaaja(t): Maija Vihinen-Ranta

Tiivistelmä:

Herpes simplex virus 1 (HSV-1) on alfaherpesviruksiin kuuluva vaipallinen, kaksijuosteista DNA:ta sisältävä virus. Kosketus- ja pisaratartuntana herkästi leviävä HSV-1 on maailmanlaajuisesti huomattava taudinaiheuttaja, sillä virusta kantaa arviolta 67 % väestöstä. Tartunta on elinikäinen. Latentissa vaiheessa HSV-1:n genomi säilyy aistihermojen hermosolmukkeissa. Viruksen aktivoituminen lyyttiseen lisääntymiskiertoon oireilee tyypillisesti rakkuloina kasvojen iholla ja limakalvoilla. HSV-1:n genomin replikoituminen ja uusien viruskapsidien muodostuminen tapahtuvat isäntäsolun tumassa, jossa viruksen rakentumisalue laajenee infektion edetessä. Samalla isäntäsolun kromatiini tiivistyy ja pakkautuu tuman reunamille. Uudet viruskapsidit poistuvat tumasta kuroutumalla tumakalvon läpi mekanismilla, joka tunnetaan jo varsin hyvin. Sen sijaan on vielä epäselvää, kuinka kapsidit saavuttavat sisemmän tumakalvon liikkuessaan kromatiinin seassa. Tässä tutkimuksessa määritettiin isäntäsolun kromatiinin ominaisuuksia ja vuorovaikutuksia viruksen kanssa lyyttisen HSV-1-infektion myöhäisessä vaiheessa. Löyhästi pakkautuneen aktiivisen eukromatiinin ja tiiviimmin pakkautuneen hiljaisen heterokromatiinin erottamiseen käytettiin vasta-ainemarkkereita, jotka sitoutuvat kromatiinin eri muodoille ominaisiin histonimodifikaatioihin. Konfokaali- ja elektronimikrokooppikuvauksen perusteella infektoituneen solun kromatiini oli tiivistynyt tuman reunoille epäsäännöllisen muotoiseksi renkaaksi. Tiivistynyttä kromatiinirengasta katkoivat paikoitellen sisemmälle tumakalvolle ulottuvat aukkokohdat, joiden kautta viruskapsidien nähtiin päätyvän tumakalvon läheisyyteen. Tiheämmän kromatiinin sekaan sijoittuneiden viruskapsidien ympärillä nähtiin elektronimikroskooppikuvauksessa usein sädekehän kaltainen tyhjä tila, joka voisi selittyä kapsidin ja kromatiinin välisillä vuorovaikutuksilla. Kromatiinin eri muotojen sijoittuminen muuttui infektiossa siten, että eukromatiinia havaittiin tumakalvon vieressä ns. periferaalisella alueella. Periferaalinen eukromatiini saattaa viitata viruksen aikaansaamiin muutoksiin geenitoiminnassa. Lyyttisellä HSV-1-infektiolla on merkittävä vaikutus isäntäsolun tumaan ja kromatiinin rakenteeseen. Kromatiinin ja viruksen välisten vuorovaikutusten tarkempi määrittäminen voi tuoda lisätietoa kapsidien tumansisäisistä vaiheista ja tarjota samalla potentiaalisia kohteita lääkemolekyyleille, joilla infektion eteneminen pyritään pysäyttämään tumaan.

Avainsanat: HSV-1, herpesvirukset, tuma, kromatiini, virus-tuma-vuorovaikutukset

Table of Contents

Abbreviations

H2B-ECFP	Fusion protein of cellular histone H2B with enhanced cyan fluorescent protein
H3K9me3	Post-translational histone modification associated with constitutive heterochromatin
H3K27ac	Post-translational histone modification associated with euchromatin
H3K27me3	Post-translational histone modification associated with facultative heterochromatin
HeLa MZ	Human adenocarcinoma cell line
HSV-1	Herpes simplex virus 1
ICP8	Infected cell protein 8, single-strand DNA-binding protein of HSV-1
NPC	Nuclear pore complex
p.i.	Postinfection
PTM	Post-translational modification
RC	Viral replication compartment
TEM	Transmission electron microscope
UL	Unique long region of HSV-1 genome
US	Unique short region of HSV-1 genome
Vero	Monkey kidney epithelial cell line
VP	Viral protein
VP26-mCherry	Fusion protein of HSV-1 capsid protein VP26 with fluorescent monomeric Cherry protein

1. Introduction

1.1 Herpes simplex virus 1 (HSV-1)

Herpes simplex virus 1 (HSV-1) is a human pathogen infecting an estimated 67 % of the global population (Looker et al., 2015). HSV-1 is commonly associated with cold sores, blistery facial lesions that form in the skin and mucosal membranes as the virus establishes lytic infection for replication and shedding (reviewed by Whitley et al., 2007). As a neurotropic virus capable of latency, HSV-1 causes a life-long infection by hiding dormant in the nuclei of sensory neurons. Sporadic reactivation episodes of latent virus lead to lytic infection and anterograde transport of progeny viruses back to the facial epithelium, the major site of productive infection.

HSV-1 requires the nuclear machineries of host cell for viral transcription, mRNA splicing, and DNA genome replication. Furthermore, progeny nucleocapsids are assembled in the nucleus. Lytic HSV-1 infection induces profound changes in nuclear architecture and size (Monier et al., 2000), chromatin distribution (Schwartz and Roizman, 1969), lamina integrity (Simpson-Holley et al., 2004a), and some nuclear organelle properties (Maul et al., 1993; (Chang et al., 2011). Alongside the structural nuclear alterations, proceeding HSV-1 infection downregulates host cell gene expression, while co-transcriptional splicing remains functional (Rutkowski et al., 2015). In addition, viral disruption of host transcription termination mechanism results in the emergence of large transcripts of multiple sequential host genes (Rutkowski et al., 2015). After nuclear replication and assembly, intact viral nucleocapsids egress from the nucleus. As their large size (125 nm) excludes nuclear export via the nuclear pore complex, progeny nucleocapsids exit by budding through the nuclear membrane – a mechanism considered to be unique for herpesviruses until recently (reviewed by Bigalke and Heldwein, 2016).

1.1.1 Genome

HSV-1 possesses a linear, double-stranded DNA genome of approximately 152 kb in size (Lehman and Boehmer, 1999; McGeoch et al., 2006; Szpara et al., 2014). The genome circularizes upon viral entry and insertion into the host cell nucleus. Most HSV-1 core genes, involved in vital virus functions such as cell entry, DNA replication, and capsid assembly, reside on the long unique sequence region (UL). Another cluster of genes, designated the short unique sequence region (US), encodes mostly non-essential proteins, such as the viral lipid envelope glycoproteins that interact with cellular receptors and immune system components, and are subject to greater evolutionary divergence among herpesviruses. Both unique sequences are flanked by a set of terminal and internal repeat sequences. The repeat sequences encode two immediately-early proteins important for lytic infection, as well as a neurovirulence factor protein, and the majority of LAT transcript, which is required for the upkeep of latent HSV-1 infection. The repeat sequence regions allow for genome recombination, during which the long and short unique sequence regions may become inverted in respect to each other. Consequently, HSV-1 genomes are eventually present in four equimolar isomers (Hayward et al., 1975) even if the viral population initiates from a single genome isomer. Flanking the genome ends, short terminal sequences facilitate genome circularization. Additionally, they contain packaging signals required for cleaving the full-length genome from a replication concatemer into a progeny nucleocapsid (McVoy et al., 2000). HSV-1 genes, out of which only four contain introns and undergo splicing, are transcribed by cellular RNA polymerase II. In total, HSV-1 genome encodes 74 known proteins (UniProt Proteome ID UP000106517, retrieved on 19.01.2017). The function of some HSV-1 proteins, including some essential proteins for productive infection, remains to be established. HSV-1 strains differ in infectivity and neurovirulence (Dix et al., 1983; Wang et al., 2013). However, the 26 sequenced HSV-1 genomes sampled worldwide show homology exceeding 90% on amino acid level (Szpara et al., 2014).

1.1.2 Virion structure

HSV-1 virion core is a nucleocapsid of 125 nm in diameter (Zhou et al., 2000). The nucleocapsid is surrounded by a protein-rich tegument, which is enveloped by a lipid membrane derived from an intracellular membrane structure of the host cell. The diameter of a mature, enveloped HSV-1 virion is approximately 200 nm.

HSV-1 capsid is assembled from seven structural proteins encoded by the long unique sequence region of the genome: VP5, VP19C, VP23, VP26, UL17, UL25, and portal protein (reviewed by Brown and Newcomb, 2011). The major HSV-1 capsid component is designated VP5. This protein forms capsomers – 150 hexamers and 12 pentamers – that lie on a T=16 icosahedral lattice (Newcomb et al., 1993). Each capsomer is surrounded by six heterotrimers, consisting of a single VP19C and two VP23, which connect adjacent capsomers. VP26 is located at the tip of each hexamer subunit, totaling in 900 copies of VP26 per capsid. Additionally, a heterodimer consisting of UL17 and UL25 is present on the capsid surface in lesser copies. A special portal protein in 12 copies forms a unique vertex structure, through which the HSV-1 genome can be packaged into an assembled capsid.

Tegument, connecting the nucleocapsid to the viral envelope, contains up to 24 different viral-encoded proteins both essential and non-essential for a successful infection (reviewed by Kelly et al., 2009), as well as minute amounts of various host cell proteins (Loret et al., 2008). The exposed outer tegument proteins detach as the virion enters the cell by fusing the viral envelope with the plasma membrane. Inner tegument proteins remain associated with the nucleocapsid, facilitating its transport to the nucleus along microtubules. Some of the detaching tegument proteins, such as virion host shutoff protein, promote infection by acting within the cytoplasm. Other tegument proteins, such as VP16, enter the nucleus and co-operate with cellular transcription factors to facilitate the transcription of viral immediate-early genes.

Viral envelope contains viral transmembrane proteins, most of which are glycosylated (Lamers et al., 2015). Out of 12 predicted HSV-1 glycoproteins, nine (gB, gC, gD, gE, gG, gH, gI, gL and gM) were detected in purified HSV-1 virions by protein mass spectrometry analysis

(Loret et al., 2008), as were four nonglycosylated membrane-associated proteins (UL20, UL45, UL56 and US9). Glycoproteins gB, gD, gH and gL are deemed essential for viral attachment and entry. Protruding viral envelope proteins appear as 600-750 spikes on the virion surface, and form clusters with an uneven, possibly functional distribution (Grunewald et al., 2003).

1.1.3 Reproductive life cycle

HSV-1 attachment and entry into a susceptible host cell is facilitated by viral envelope glycoproteins interaction with the extracellular matrix components and the cell surface receptors, such as nectin-1 (reviewed by Kukhanova et al., 2014). HSV-1 viral particles can enter the cell by fusion of viral envelope with the plasma membrane, or via a special endocytic pathway. Naked nucleocapsid, with attached tegument proteins, is transported to the nuclear envelope, where it docks into a nuclear pore complex, resulting in the nuclear ejection of viral genome. The nuclear genome circularizes (Poffenberger and Roizman, 1985; Strang and Stow, 2005), and it is chromatinized by cellular histones (Kent et al., 2004). Viral genes are then transcribed by cellular RNA polymerase II (Alwine et al., 1974) as a self-regulatory cascade. Immediately-early gene products function to promote the production of early gene proteins, which facilitate viral DNA replication. Late gene products are mainly structural proteins required for the assembly of progeny capsids, tegument layers, and viral membranes. HSV-1 genome replication and recombination yields concatemeric DNA, which contains multiple HSV-1 genomes in a single DNA molecule (Jacob and Roizman, 1977). In viral replication compartment (RC) area, a full-length genome is then cleaved and reeled into an assembled capsid, guided by the packaging signals present on the DNA sequence. Mature nucleocapsids have been shown to move by passive diffusion towards the nuclear borders (Bosse et al., 2014). Upon reaching the nuclear envelope, nucleocapsids bud through the inner nuclear membrane into the perinuclear lumen, acquiring the primary viral envelope (Skepper et al., 2001). Fusion of primary viral envelope with the outer nuclear membrane subsequently releases the nucleocapsids into the cytoplasm (Skepper et al., 2001). The secondary viral envelope is acquired as the nucleocapsids bud into the *trans*-Golgi network or an endosome at the sites of embedded viral membrane proteins. The layer of tegument proteins around a

nucleocapsid forms gradually prior to both envelopments (reviewed by Guo et al., 2010). Enveloped viral particles are then transported to the plasma membrane in a vesicle, and released by exocytosis. HSV-1 latency is established as the virus enters the dendrite of the trigeminal, facial, or vestibular neuron, and is retrogradely transported to the nucleus. Viral genome (typically 1–100 copies per nucleus) persists as circularized episome (Rock and Fraser, 1983) in a chromatinized state (Deshmane and Fraser, 1989). Viral gene expression during latency is limited to abundant production of the latency-associated transcript (LAT), which suppresses lytic HSV-1 genes, and possibly promotes host cell survival by inhibiting apoptosis (Nicoll et al., 2012).

1.2 Nucleus

The eukaryotic nucleus functions as a limited-access storage for genetic information. The major processes within the nucleus are controlled transcription and the generation of mature transcripts, as well as the maintenance and replication of the genome. Structurally, the nucleus is defined by the nuclear envelope, which consists of the inner and outer nuclear membranes. Spanning both membranes, nuclear pore complexes (NPC) allow for bidirectional diffusion of ions and small molecules up to 9 nm, and active transport of larger proteins up to 39 nm in size (Pante and Kann, 2002). A network of lamins, a family of intermediate filaments, forms a thin layer beneath the nuclear envelope. This layer, designated the nuclear lamina, provides anchorage points for the chromatin, and is a major contributor to the shape and structural integrity of the nucleus (reviewed by Goldman et al., 2002). Nuclear interior lacks membrane-based compartmentalization. Rather, intranuclear organelles exist in the nucleoplasm as dynamic protein aggregates that form around a crucial matrix protein characteristic for each organelle. The function of most intranuclear organelles is not fully understood, however, they are generally considered biochemical factories or storage sites related to transcription, or splicing and other post-transcriptional editing of immature transcripts (Zimber et al., 2004).

1.2.1 Chromatin

Nuclear DNA is condensed into DNA-protein complex called chromatin (Davies and Small, 1968; reviewed by Annunziato, 2008). This arrangement compacts long DNA molecules, and provides a level of regulation by affecting the accessibility of different genome segments. The core unit of chromatin is the nucleosome, a disc-like histone protein octamer, around which DNA wraps 1.65 times (Luger et al., 1997). Histones are small, basic proteins that bind strongly to the negatively charged DNA through electrostatic interactions. The nucleosome consists of canonical histones H2A, H2B, H3, and H4, each present in two copies. Nucleosomes are stabilized by the addition of the linker histone H1, and connected by short (~200 bp) segments of linker DNA. The long chain of repeating nucleosomes is compressed into densely looped chromatin fiber (Robinson et al., 2006). Chromatin is a dynamic structure. Transient displacement and reassembly of histones enable transcription, DNA replication and repairing, and genetic recombination processes (Venkatesh and Workman, 2015). Furthermore, minor histone variants and covalent histone modifications alter the chemical and physical properties of the chromatin fiber, resulting in variable interactions with chromatin-binding components.

1.2.1.1 Epigenetic regulation by histone post-translational modifications

Histone post-translational modifications (PTMs) traditionally refer to acetylation, methylation, and phosphorylation of histones either on their protruding N-terminal tails, or the globular core domains (Allfrey et al., 1964; reviewed by Bannister and Kouzarides, 2011). The growing list of novel histone PTMs includes the conversion of arginine residues into citrulline, the addition of β-N-acetylglucosamine or ADP-ribose, ubiquitylation and SUMOylation, and the clipping of histone tails (reviewed by Bannister and Kouzarides, 2011). Some modifications are thought to alter chromatin structure directly by neutralizing charged amino acid residues on histones, or by hindering the interaction of adjacent nucleosomes. On the contrast, the addition of small chemical groups that do not affect the charge can provide a platform for DNA-binding proteins, or inhibit the interaction between a histone and a binding partner. Histone PTMs are mechanisms that regulate epigenetic phenomena by promoting or blocking

the accessibility of the genetic data stored into DNA sequences. Most histone PTMs are reversible. The modifications are a function of the local concentration of the modifying enzymes and key metabolites, thus linking gene expression to environmental factors. Chromatin regions with differing structure and certain characteristic histone PTMs are classified as active euchromatin and silent heterochromatin, depending on the level of transcriptional activity.

1.2.1.2 Euchromatin and heterochromatin

Euchromatin is transcriptionally active chromatin region that contains most of the expressing genes (reviewed by Bannister and Kouzarides, 2011). The characteristic histone PTM of euchromatin is the acetylation of lysine residues, such as histone H3 acetylation of lysine on amino acid position 27 (H3K27ac) (Suka et al., 2001). Acetylation counters the positive charge of lysine, weakening the electrostatic interaction between the histone core and the bound, negatively charged DNA. This is thought to result in less compacted chromatin, and easier nucleosome displacement for transcription. Hyperacetylation, involving multiple lysine residues on histone tails, is typically found on gene promoters, presumably to enhance the binding of transcription factors. On the contrast, heterochromatin is highly condensed chromatin with diminished transcriptional activity. Heterochromatin regions are further divided into constitutive and facultative heterochromatin. Constitutive heterochromatin contains permanently silent genes, includes regions such as telomeres, and is characterized by histone H3 trimethylation PTM of the lysine on amino acid position 9 (H3K9me3) (Shi and Dawe, 2006). The genes of facultative heterochromatin are active during cellular differentiation or during a development stage of the organism, and become silenced thereafter. Facultative heterochromatin, such as the inactivated X-chromosome of mammalian females, is typically enriched with another histone H3 trimethylation PTM of the lysine on amino acid position 27 (H3K27me3) (Tie et al., 2009).

2. Aims of the study

Three major alterations in the nuclear architecture of an infected cell in late infection include the growth of nuclear size, the formation of viral RCs, and the marginalization of host chromatin. RCs are the site of viral transcription, genome replication, and the assembly of progeny nucleocapsids. As the nuclear volume occupied by RCs increases, host chromatin is condensed and distributed to the nuclear periphery. Within this environment, progeny nucleocapsids need to reach the nuclear envelope egress site. In order to gather more information on virus–nucleus interactions in late HSV-1 infection, the aims of this study were:

I To study the host chromatin redistribution, especially in relation to RCs and intranuclear progeny nucleocapsids.

II To study the positioning of active and silenced host chromatin regions, identified by histone PTMs.

3. Materials and methods

3.1 Cell lines and viruses

Mouse B cells immortalized with Abelson murine leukemia virus (a generous gift from Barbara Panning, University of California, San Francisco, USA) and human B cells (cell line GM12878, Coriell Cell Repositories) were cultured as suspension in RPMI 1640 growth medium (Gibco, Life Technologies) supplemented with 1% L-glutamine, 1% penicillin-streptomycin, and 10% or 15% fetal bovine serum, respectively. The B cells were passaged by dilution into the density of 300 000 cells/ml once a week. HeLa MZ cells were cultured as monolayers in DMEM GlutaMAX growth medium (Gibco, LifeTechnologies) supplemented with 10% fetal bovine serum, 1% penicillin-streptomycin, and 1% non-essential amino acids. HeLa cell line expressing the fluorescent hybrid histone protein H2B-ECFP was created by transfecting HeLa MZ cells with the plasmid construct by Dr. Jörg Langowski (German Cancer Research Center, Division Biophysics of Macromolecules, Germany) using transfection reagent kit Lipofectamine 3000 (Invitrogen) according to the manufacturer's instructions. Transfected cells were selected by the addition of 0.5 mg/ml G418-containing Geneticin (Gibco, Life Technologies). HeLa MZ and HeLa H2B-ECFP cell lines were passaged 1:6 or 1:8 twice a week. Vero cells were cultured as monolayers in DMEM GlutaMAX growth medium (Gibco, LifeTechnologies) supplemented with 10 % fetal bovine serum and 1% penicillin-streptomycin, and passaged 1:10 twice a week. All cell lines were incubated in a humidified atmosphere at 37°C with 5% carbon dioxide. Wild-type HSV-1 strain 17+ stored in milk stock was a kind gift from Dr. Veijo Hukkanen (University of Turku, Finland). HSV-1 strain expressing the fluorescent hybrid capsid protein VP26-mCherry was a kind gift from Dr. Beate Södeik (Institute of Virology, Hannover Medical School, Germany). Additional virus batch of HSV-1 VP26-mCherry was produced in Vero cells by inoculating 70–80% confluent Vero cultures at an MOI of 0.01. Virus was harvested after four days by lysing the cells with three cycles of freezing and thawing, after which the lysed cells were pelleted (1500 rpm/3 min) and resuspended into sterile 9% skimmed milk. Despite of repeated attempts, determining the viral titer failed, and the PFU value of the original virus was used as an estimated PFU value of the new virus batch.

3.2 Transmission electron microscopy studies

Mouse B cells, human B cells, and Vero cells grown on coverslips were infected with wild-type HSV-1 strain 17^+ at an MOI of 5. Infected cells were incubated in humidified atmosphere at 37°C with 5% carbon dioxide, and fixed at 16 h, 20 h, or 24 h post infection (p.i.) by storing the cell samples into fixative containing 0.25% glutaraldehyde and 4% paraformaldehyde. Vero cells were washed with 50 mM phosphate buffer (pH 6.8) prior to fixation. The B cells were pelleted (11 g / 10 min) after the initial 20 min fixation time in order to remove and replace the initial fixative suspension (0.5% glutaraldehyde and 8% paraformaldehyde diluted 1:1 into the cell suspension). Fixed cell samples were post-fixed with 1% osmium tetroxide for 1 h on ice, dehydrated in a rising ethanol series, and embedded into Low-viscosity embedding resin (TAAB Laboratories Equipment Ltd., UK). Thin sections were cut with UltraCut UC6A ultramicrotome (Leica Mikrosysteme GmbH, Germany), and transferred onto Pioloform-coated single-slot copper grids. Finally, the grids were stained with 2% aqueous uranyl acetate and lead citrate. Post-fixation and all subsequent transmission electron microscopy (TEM) sample preparation steps were performed by Mervi Lindman (Electron Microscopy Unit, Institute of Biotechnology, University of Helsinki, Finland). The samples were imaged with JEOL JEM 1400 (JEOL Ltd., Japan) transmission electron microscope equipped with bottom-mounted Quemesa CCD camera (4008 x 2664 pixels). High voltage of 80 kV was used for imaging.

3.3 Immunolabeling studies

Human B cells, Vero cells, and HeLa MZ cells plated on coverslips were infected with wild-type HSV-1 strain 17^+ at an MOI of 5. Infected cells were incubated in humidified atmosphere at 37°C with 5% carbon dioxide, and fixed at 24 h p.i. with 4% paraformaldehyde for 20 minutes in RT. Prior to fixation, the B cells were pelleted (11 g/5 min), resuspended into 20 µl of growth medium, transferred onto coverslips, and air-dried for 10–15 minutes. An additional series of HSV-1 infected HeLa MZ cell samples was similarly prepared, and fixed at 12 h, 14 h, 16 h, 18 h, 20 h, and 24 h p.i.

Human B, Vero, and HeLa MZ cell samples fixed with paraformaldehyde at 24 h p.i. were separately immunolabeled for the euchromatin marker H3K27ac (primary rabbit antibody Abcam 4729, dilution 1:350, Abcam, Cambridge, UK), the constitutive heterochromatin marker H3K9me3 (primary rabbit antibody Abcam 8898, dilution 1:1000, Abcam, Cambridge, UK), and the facultative heterochromatin marker H4K20me3 (primary rabbit antibody Abcam 9053, dilution 1:1000, Abcam, Cambridge, UK). All samples were additionally labeled for the major HSV-1 capsid protein VP5 (primary mouse monoclonal antibody against VP5, dilution 1:200, Santa Cruz Biotechnology Inc. Dallas, TX, USA) to reveal the infected cells. The time point series of infected HeLa MZ cell samples was labeled for the HSV-1 single-stranded DNA-binding protein ICP8 (monoclonal antibody, dilution 1:100, Novus Biologicals, Littleton, CO, USA) to reveal the viral replication compartment regions. Alexa-conjugated secondary antibodies (dilution 1:200) against rabbit (Alexa 633, Thermo Fisher Scientific, Massachusetts, USA) and mouse (Alexa 488, Thermo Fisher Scientific, Massachusetts, USA) were used respectively. Immunolabeling was done with infiltration buffer containing 0.1% sodium azide, 0.1% Triton-X, and 0.5% (w/v) bovine serum albumin in phosphate buffered saline. Antibody dilutions were prepared into the infiltration buffer. Labeled coverslips were mounted on glass slides with ProLong Gold antifade reagent with DAPI (Thermo Fisher Scientific, Massachusetts, USA). Samples were imaged with Olympus FV1000 laser scanning confocal microscope using UPLSAPO 60x (N.A. 1.35) oil immersion objective. DAPI was excited with a 405 nm diode laser, and emission was collected with a 450/50-nm band-pass filter. Alexa 488 was excited with a 488 nm argon laser and fluorescence was collected with a 515/30 nm band-pass filter. Alexa 633 was excited with a 633 nm He-Ne laser and the fluorescence was collected with a 647 nm long-pass filter. Image size was between 512 x 512 and 1600 x 1600 pixels with a pixel resolution of 66–69 nm.

3.4 Live cell imaging

HeLa H2B-ECFP cells were grown on live plates to 70–80% confluency, and infected with HSV-1 VP26-mCherry at an estimated MOI of 5. The cells were incubated in humidified atmosphere at 37 °C with 5% carbon dioxide for the first six hours, after which the infection

medium was replaced with fresh medium. The cell plate was then inserted into the pre-warmed live cell chamber (37 °C, oxygen supply with 5% carbon dioxide) of Nikon A1R laser scanning confocal microscope (Nikon Instruments Inc., Melville, USA). The cells were imaged using CFI Plan Apo VC 60x (N.A. 1.2, WD 0.31-0.28) water immersion objective. The fluorescent label ECFP was excited with a 405 nm diode laser, and emission was collected with a 450/50 nm band-pass filter. The fluorescent label mCherry was excited with a 561 nm sapphire laser, and emission was collected with a 595/50 nm band-pass filter. A series of images was recorded between 7 h and 24 h p.i. with an interval of 10 minutes. In order to decrease the cytotoxic effect of the excitation lasers, a low-resolution overview image of ~30 cells was captured at 10 min intervals between 7 h and 24 h p.i. The experiment was a co-operation with Master's degree student Apurba Majumder (Nanoscience Center, University of Jyväskylä, Finland).

3.5 Processing of image data

Confocal images were processed with ImageJ. Brightness and contrast were adjusted automatically (Image → Adjust → Brightness/Contrast → Auto), and the image channels were merged (Image → Color → Channels tool → Merge channels). Images were cropped and arranged into panels using Irfan View and MS Paint image software.

4. Results

4.1 Redistribution of host chromatin in late infection

To analyze the redistribution of host chromatin, we examined HSV-1 infected cells by TEM. Imaging verified the presence of progeny nucleocapsids in the nuclei of mouse B (Fig. 1A), human B (Fig. 1B, and Vero cells (Fig. 1C). At the same time, an increase in nuclear volume and altered chromatin distribution was detected in all three cell lines. Most of the chromatin was found at the nuclear periphery in electron-dense chromatin rifts, which extended to the nuclear envelope. The condensed chromatin did not typically form an evenly distributed, marginalized chromatin ring. Rather, the condensed chromatin rifts varied in density, thickness, and were, in most nuclei, spaced by irregularly-sized gaps devoid of dense chromatin (Fig. 1A and 1C). These low-density chromatin gaps appeared to be continuous with the central electron-luscent region. The gaps were frequently distributed in an NPC-independent manner, and they were often remarkably wider than the NPC-associated channels seen in non-infected nuclei (Fig. 2). HSV-1 nucleocapsids were frequently observed to locate in the low-density gaps (Fig. 1B and 1C), indicating that the gaps were sufficiently sparse to allow for nucleocapsid egress from the central nucleus to the inner nuclear membrane

TEM micrographs of non-infected mouse B (Fig. 2A), human B (Fig. 2B), and Vero cells (Fig. 2C) showed the chromatin distribution in interphase nuclei. The loosely packaged and transcriptionally active euchromatin was seen as the electron-luscent areas in the central regions of the nuclei as described in literature. Heterochromatin appeared as electron-dense areas, which were especially prominent at the nuclear periphery. NEC-associated low-density channels were seen spanning the layer of dense heterochromatin at nuclear periphery (Fig. 2 insets).

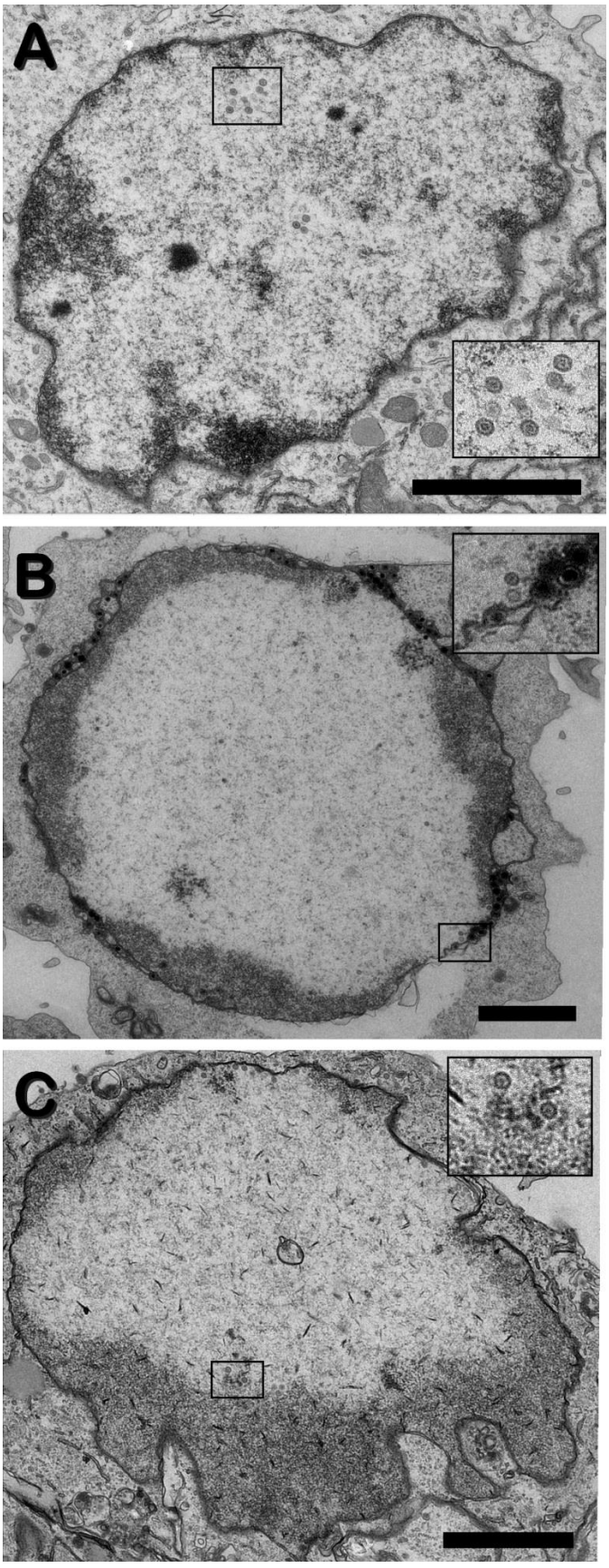

Figure 1: Distribution of host chromatin and HSV-1 nucleocapsids in late infection. TEM micrographs of mouse B cell (A), human B cell (B), and Vero cell (C) nuclei in late HSV-1 infection. Viral replication compartments were seen as electron-luscent central regions, which contained progeny nucleocapsids (insets). Host chromatin was condensed and marginalized to the nuclear periphery. Replication compartments formed gaps through the layer of host chromatin, which allowed for the nucleocapsids to contact the inner nuclear membrane for nuclear egress. Scale bars, 2 μm.

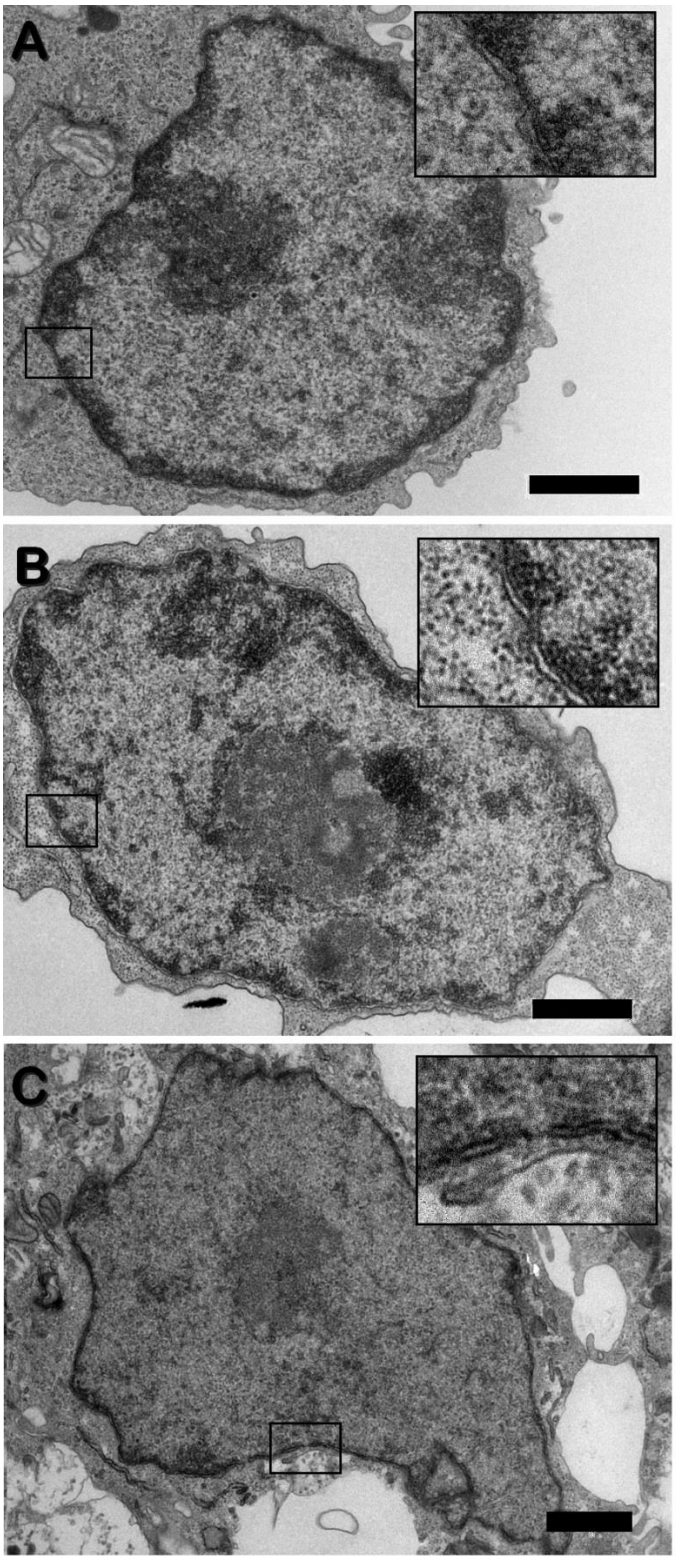

Figure 2: Distribution of chromatin in non-infected control nuclei. TEM micrographs of mouse B cell (A), human B cell (B), and Vero cell (C) nuclei at interphase. Nuclear interior was filled with evenly distributed, electron-luscent material, likely corresponding to active euchromatin. Electron-dense regions at the nuclear periphery suggested densely packaged heterochromatin, which was breached at the site of nuclear pores (insets). Scale bars, 1 μm.

4.2 Redistribution of host chromatin in relation to viral replication compartments

Marginalization of host chromatin is accompanied by the expansion of intranuclear HSV-1 RCs, which were located in the electron-luscent regions in TEM micrographs. In order to observe the relative localization of confirmed HSV-1 RC regions within the host chromatin, infected HeLa cells were immunolabeled for the viral RC-associated protein ICP8, and the host chromatin was stained with DAPI. To study the possible development of viral RCs, and host chromatin redistribution in late infection, infected samples were fixed as a time point series ranging from 12 to 24 h p.i. with a two-hour interval (Fig. 3). A minimum of 30 nuclei were imaged for each time point. At 12 and 14 h p.i., a typical infected nucleus was enlarged and divided into compartments, which were filled with viral RCs, and framed by condensed chromatin. RCs appeared to be in the process of merging, as suggested by the narrow extensions connecting adjacent RCs. However, a few nuclei contained a large, intact RC region at 12 h p.i. As synchronized infection was not used for this experiment, these cells may have been the first to be infected, and had proceeded to the late stage of infection. In a typical nucleus, most chromatin was compressed into the nuclear center or into one side of the nucleus, likely reflecting the combined effect of all RC areas, which varied in their initial positioning. At the same time, marginalized chromatin at the nuclear periphery formed a ring, which was not uniform in density, but contained short gap-like segments of sparse chromatin. RCs generally extended to the peripheral chromatin ring at 12 h p.i., and appeared to breach the chromatin layer at the sites of sparse chromatin, although it was not possible to tell when the RCs established a direct contact with the inner nuclear membrane. Low-density gaps in the peripheral chromatin ring were obvious at 16 h p.i. in the nuclei that contained 1-2 large RCs. The nuclei later in infection displayed characteristics similar to the nuclei at 16 h p.i. Most of the chromatin remained compressed into the central or a side region of the nuclei. The peripheral chromatin ring remained detectable but discontinuous, apparently breached by RCs.

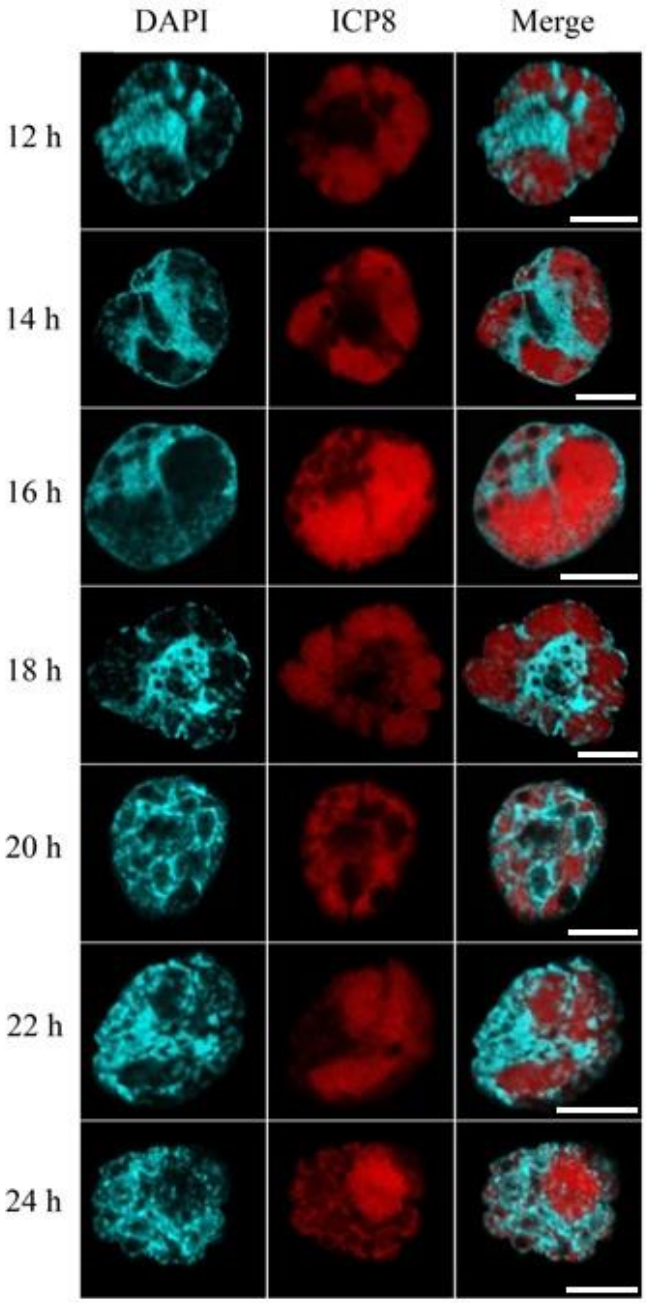

Figure 3: Development of HSV-1 replication compartments in late infection. HSV-1 infected HeLa cell nuclei. Samples were fixed at a two-hour interval between 12–24 h p.i. Nuclear staining of viral single-strand DNA-binding protein ICP8 (red) revealed the replication compartment region. Host chromatin stained with DAPI (cyan) was often partially condensed to the nuclear interior, and partially marginalized to the nuclear periphery. Replication compartments appeared to extend to the nuclear periphery at the sites of sparse chromatin already at 12 h p.i. Sparse chromatin gaps at the nuclear periphery became more obvious at 16 h p.i. Nuclear changes observed after 18 h p.i. might have been signs of nuclear degradation due to infection. Scale bars, 10 μm.

Starting from 18 h p.i., and increasing at each time point thereafter, the largest infected nuclei often appeared fragmented, cloverleaf-shaped, and sometimes disintegrated by cavities that extended to the nuclear envelope. DAPI staining in some of these nuclei was faint, indicating throughout DNA fragmentation. The remarkable changes in chromatin architecture starting from 18 h p.i. might have been signs of nuclear damage or apoptosis induced by prolonged

viral infection. Notably, round spots excluding both chromatin and ICP8 were visible at all time points. The spots might have represented regions of highly concentrated viral components, possibly clusters of progeny HSV-1 nucleocapsids. Another explanation could be the presence of fragmented nucleoli, as herpesvirus infection is known to induce disintegration of the nucleoli (reviewed by Salvetti and Greco, 2013).

4.3 Redistribution of host chromatin in relation to progeny nucleocapsids

Late HSV-1 infection is characterized by the transcription and translation of late viral genes, which includes the production of capsid proteins. The capsid proteins are translocated to the nucleus, where progeny nucleocapsids are assembled and packaged with viral DNA. Nuclear egress of mature nucleocapsids is thought to occur through low-density gaps and narrow channels, which breach the marginalized peripheral chromatin (Simpson-Holley et al., 2005; Myllys et al., 2016). Here, we used HeLa cells with fluorescently labeled histone H2B, and HSV-1 VP26-mCherry for live cell imaging to gain more information on the interaction of nucleocapsids and host chromatin (Supplementary video 1). Based on the nuclear accumulation of VP26, roughly two thirds of the cells were asynchronously infected with HSV-1, and entered the late stage of infection between 7 and 20 h p.i. Imaging of seven infected cells indicated subpopulations of high and low VP26 signal intensities. In the cells with a high VP26 intensity, VP26 was seen in the nucleus as a bright, globular region as the infection progressed. Unfortunately, it was not possible to distinguish assembled nucleocapsids from diffuse intranuclear VP26 protein. Non-infected cells continued cell divisions through the imaging, indicating the imaging conditions supported normal cellular functions. Figure 4 shows chromatin redistribution and the localization of VP26 in a typical infected cell at late infection. Due to asynchronous infection, the actual infection starting point was unknown for this cell, and the timestamps refer to the relative time between images. The separate regions devoid of chromatin were likely occupied by RCs. The chromatin bordering RCs was partially marginalized to the nuclear periphery, and partially condensed into chromatin islets that remained in the nuclear interior. The islets seemed to form from chromatin that was trapped between adjacent, expanding RCs. VP26 signal was initially seen

as separate spots of varying intensity, which coalesced into larger regions of a high signal intensity. Notably, the initial intranuclear VP26 signal often appeared as a ring at the periphery of each separate RC region, although this phenomenon was difficult to observe in the smallest RCs due to low image resolution.

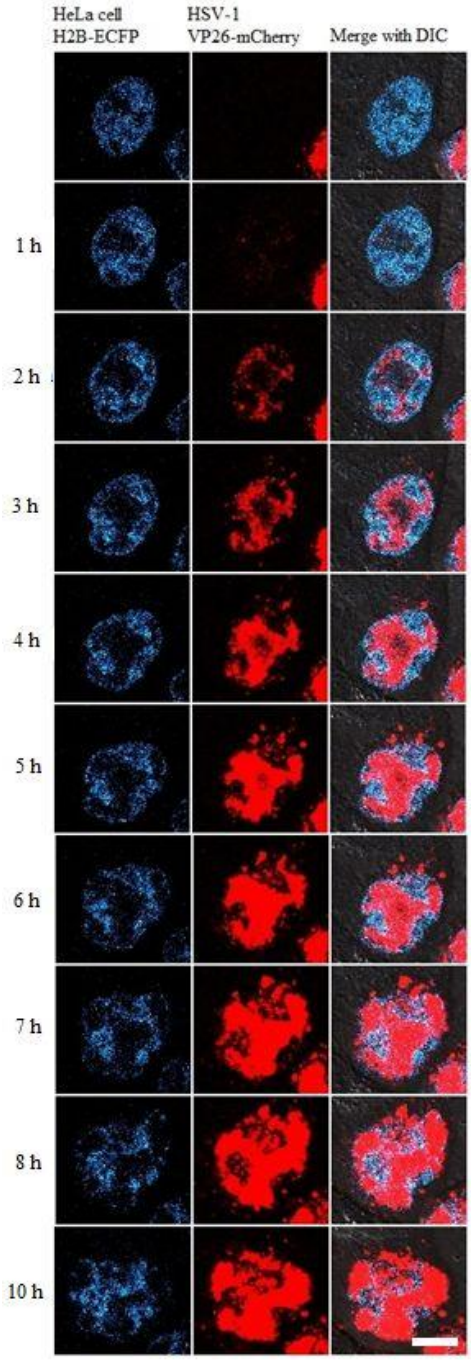

Figure 4: Intranuclear accumulation and distribution of HSV-1 capsid protein VP26. Live cell imaging data showing a HeLa cell expressing fluorescent hybrid protein histone H2B-ECFP (cyan). Cells were infected with HSV-1 expressing fluorescently tagged viral capsid protein VP26 (red). Time points are relative to the first image. The expansion of viral replication compartments, nuclear enlargement, and host chromatin condensation appeared to continue after the intranuclear accumulation of VP26. Cytoplasmic VP26 was detected within three hours following its intranuclear appearance, indicating that progeny nucleocapsids were able to egress from the nucleus through the marginalized host chromatin. Scale bar, 10 μm.

RC regions were nearly saturated with VP26 within 4 hours following the nuclear appearance of the VP26 signal. The spreading of VP26 initially excluded the islets of condensed host chromatin, likely due to their greater density that hindered the movement of HSV-1 nucleocapsids. However, separate spots of VP26 were eventually seen among the condensed chromatin islets. This might suggest ongoing rearrangement of the host chromatin as the nuclear size and the number of viral nucleocapsids increase. The phase of major nuclear enlargement was concurrent with the accumulation of VP26. Further host chromatin condensation, and the outward expansion of the nuclear edge, were seemingly driven by the growing VP26 regions.

Cytoplasmic VP26, likely indicating the nuclear egress of progeny nucleocapsids, was clearly detected within 3 hours after the nuclear appearance of the newly synthesized VP26. Due to the resolution limit used in this experiment, only the most profound changes in the integrity of the marginalized host chromatin ring could be observed. Segments of less dense chromatin at the nuclear periphery became obvious only after 1–2 hours following the appearance of the cytoplasmic VP26 signal, implicating that HSV-1 nucleocapsids were able to cross the chromatin barrier and access the nuclear envelope through gaps or channels that were too narrow or transient to be detectable in these data.

4.3.1 Individual nucleocapsids among host chromatin

The microenvironment of individual intranuclear HSV-1 nucleocapsids was studied by TEM in mouse B cells, human B cells, and Vero cells. Nucleocapsids were generally located within the low-chromatin area, although some nucleocapsids were occasionally seen among the dense peripheral chromatin. Most, but not all, nucleocapsids appeared to be surrounded by an empty interchromatin space, which ranged from corridor-like areas housing multiple nucleocapsids to a symmetrical empty halo around a single nucleocapsid (Fig. 5A and 5B). In some cases, an interchromatin corridor with multiple nucleocapsids seemed to form as a fusion of the halo-like spaces surrounding adjacent nucleocapsids (Fig. 5C). In conclusion, intranuclear HSV-1 nucleocapsids were frequently positioned into interchromatin cavities, which were often shaped after the contour of the nucleocapsid, and separated the nucleocapsid edge from host

chromatin by an approximated distance of 10–20 nm or more.

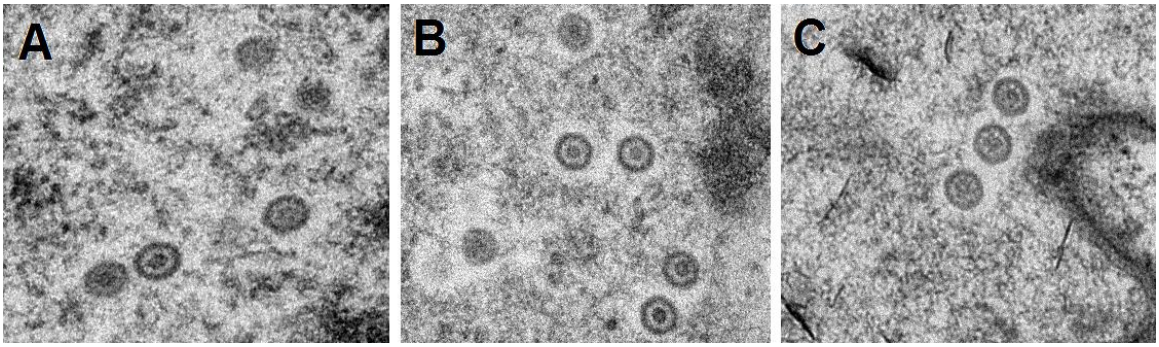

Figure 5: Intranuclear HSV-1 nucleocapsids among host chromatin. TEM micrographs showing progeny HSV-1 nucleocapsids in mouse B cell (A), human B cell (B), and Vero cell (C) nuclei. Nucleocapsids were typically seen in interchromatin gaps. At minimum, the nucleocapsid border was separated from host chromatin by a symmetrical halo-like space surrounding the nucleocapsid. Adjacent nucleocapsids appeared to form larger channels as a result of merging halos. Nucleocapsid diameter, 125 nm.

4.4 Distribution of active and silenced chromatin in late infection

Host chromatin consists of loose, transcriptionally active euchromatin, and dense heterochromatin, which contains non-coding DNA and silenced genes. We immunolabeled the histone PTMs corresponding to euchromatin, facultative heterochromatin and constitutive heterochromatin in order to study their distribution in late HSV-1 infection. Cells with late HSV-1 infection were identified by the intranuclear presence of capsid protein VP5 (data not shown). As expected, all histone PTMs displayed altered distribution in infected nuclei as a result of host chromatin condensation and marginalization. Euchromatin marker H3K27ac in infected nuclei (Fig. 6A) often formed narrow lines, which appeared to border the nuclei and individual RCs. These euchromatin borders appeared continuous, but adjacent sections varied in signal intensity in a manner that did not fully reflect the intensity of the DAPI stain. Merged images suggest that the bordering euchromatin extended up to the nuclear periphery. Euchromatin in non-infected control nuclei (Fig. 6B) was evenly distributed, granular, and excluded the nucleoli. Continuous stretches of peripheral heterochromatin appeared to separate euchromatin from the nuclear periphery at least on some regions along the nuclear perimeter. Constitutive heterochromatin marker H3K9me3 formed a thin layer at the nuclear

periphery both in HSV-1 infected nuclei (Fig. 7A) and in non-infected control nuclei (Fig. 7B). Notably, the intensity of the heterochromatin marker at the nuclear periphery did not always correlate with the intensity of DAPI stain in infected nuclei, suggesting that the seemingly sparse chromatin gaps revealed by DAPI staining might still contain a narrow layer of heterochromatin barrier of significant density. Facultative heterochromatin marker H4K20me3 in infected nuclei (Fig. 8A) was distributed similarly to the euchromatin marker, forming condensed lines along the marginalized chromatin at the nuclear periphery. Likewise, facultative heterochromatin in non-infected nuclei (Fig. 8B) resembled euchromatin in a grainy, even distribution. Small spot-like regions of high facultative heterochromatin marker intensity in non-infected nuclei might have represented clusters of silenced genes.

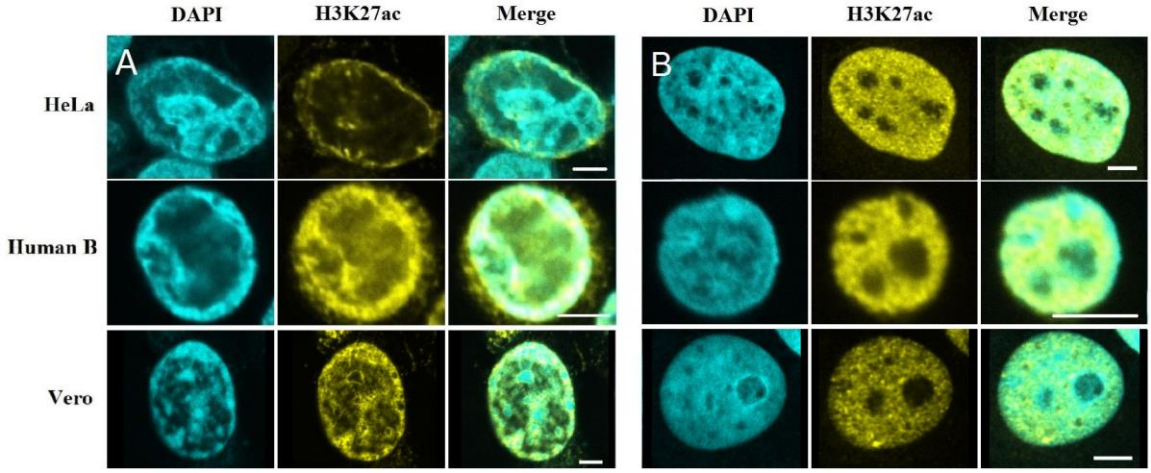

Figure 6: Distribution of transcriptionally active euchromatin in late HSV-1 infection. The nuclei of HeLa cell, human B cell, and Vero cell infected with HSV-1 (A). Infected cells were identified by the intranuclear presence of HSV-1 capsid protein VP5 (data not shown). Host chromatin stained with DAPI (cyan) was condensed, marginalized, and frequently formed dense chromatin islets in the nuclear interior. Histone post translational modification H3K27ac (yellow) was used to label euchromatin, which was seen to localize to the nuclear periphery upon infection. Non-infected control nuclei (B) displayed a grainy, rather even distribution of euchromatin in the nuclear interior. The regions lacking the euchromatin label were likely nucleoli. Merged images revealed continuous chromatin stretches not stained by the euchromatin label at the nuclear periphery, and around the nucleoli. Scale bars, 5 μm.

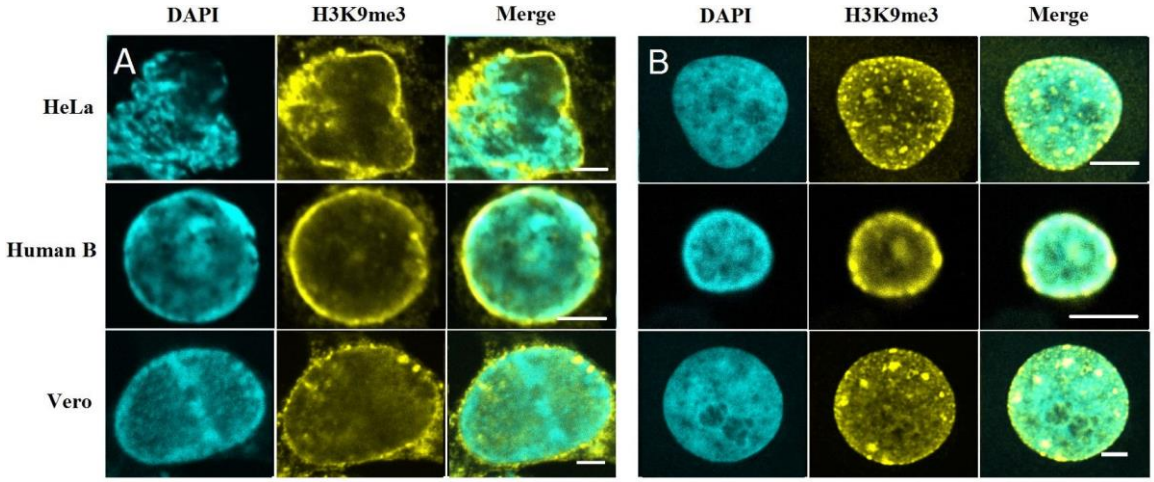

Figure 7: Distribution of transcriptionally inactive constitutive heterochromatin in late HSV-1 infection. The nuclei of HeLa cell, human B cell, and Vero cell infected with HSV-1. Infected cells were identified by the intranuclear presence of HSV-1 capsid protein VP5 (data not shown). Host chromatin stained with DAPI (cyan) was seen to condense partially to the nuclear periphery, partially into the nuclear interior. Histone post translational modification H3K9me3 (yellow) was used to label constitutive heterochromatin. A marginalized ring of constitutive heterochromatin was present at the nuclear periphery. Host chromatin stained with DAPI (cyan) displayed intensity differences at the nuclear periphery, presumably reflecting differences in chromatin density. However, constitutive heterochromatin label revealed a layer of chromatin, which was not in agreement with the chromatin density differences suggested by DAPI staining. Scale bars, 5 μm.

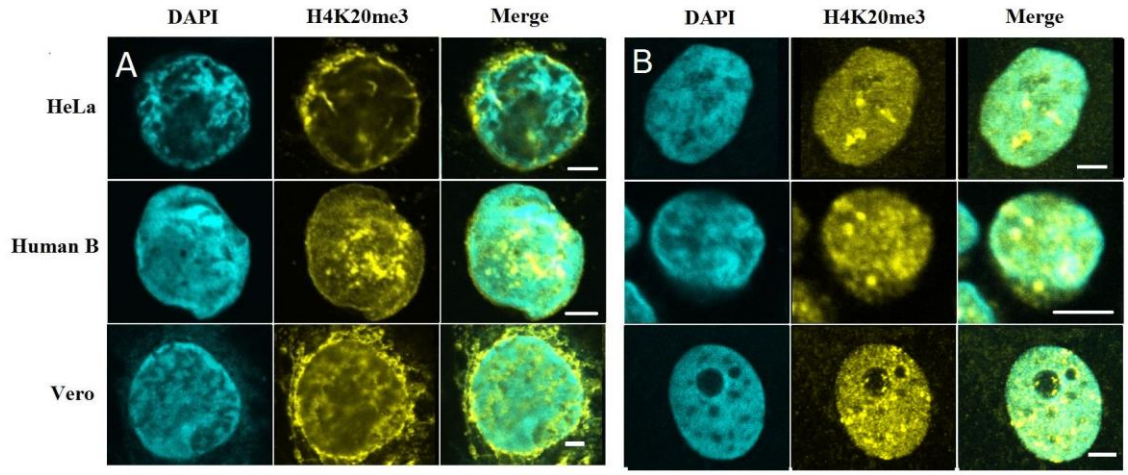

Figure 8: Distribution of transcriptionally inactive facultative heterochromatin in late HSV-1 infection. The nuclei of HeLa cell, human B cell, and a Vero cell. Infected cells were identified by the intranuclear presence of HSV-1 capsid protein VP5 (data not shown). Chromatin was stained with DAPI (cyan). Histone post translational modification H4K20me3 (yellow) was used to label facultative heterochromatin, which was seen to condense and marginalize in HeLa and Vero nuclei compared to the even intranuclear distribution in non-infected control nuclei. Occasional bright spots of H4K20me might correspond to clusters of silenced genes. Scale bars, 5 μm.

5. Discussion

Lytic HSV-1 infection induces profound changes in nuclear size and architecture. Here, we studied three interacting components of late HSV-1 infection: host chromatin, viral replication compartments, and progeny nucleocapsids. Live cell imaging of HSV-1 infected HeLa cells revealed the progress of chromatin displacement and nuclear expansion. Viral capsid protein VP26 proceeded to fill the expanding RCs, after which RCs reached their maximum size, displacing host chromatin. Likewise, nuclear enlargement was still in process, and even appeared to reach the most prominent phase following the intranuclear accumulation of progeny nucleocapsids. In HEp-2 cells, the cross-sectional area of infected nuclei doubles, with the nuclear enlargement phase detectable from 8 to 16 h p.i. (Simpson-Holley et al., 2005). Determination of exact time points was challenging due to asynchronous infection in our experiment setting with HeLa cells. However, the obviously visible phase of nuclear enlargement continued for roughly 7 hours in HeLa cells, which is comparable with the previous result in HEp-2 cells (Simpson-Holley et al., 2005). Nuclear enlargement and RC maturation to the nuclear periphery both depend on viral proteins UL31 and UL34, which disrupt the nuclear lamina (Simpson-Holley et al., 2004b), and form the viral nuclear egress complex on the inner nuclear membrane. Even though nuclear lamina disruption by UL31 and UL34 is essential for nuclear enlargement, the timing of events suggests that intranuclear accumulation of progeny nucleocapsids might promote RC maturation, and indirectly contribute to the increase in nuclear volume, and to host chromatin condensation.

We additionally studied host chromatin marginalization in fixed samples of HSV-1 infected HeLa cells, Vero cells, and B lymphoblastoid cells from human and mouse. TEM samples provided a closer look at marginalized host chromatin in late HSV-1 infection. The nuclei showing electron-dense chromatin packed at the nuclear periphery corresponded well with the final phase of chromatin condensation described by Monier et al. (2000). Irregularly-shaped islets of condensed chromatin near to the central nuclear region likely represented the original borders of separate RCs. As early RCs undergo directed movement, expand and coalesce at nuclear speckles to form large, globular regions of viral biosynthesis that exclude host

chromatin (Taylor et al., 2003; Chang et al., 2011), host chromatin might become partially trapped between adjacent RCs.

Other nucleus-replicating viruses known to induce host chromatin marginalization include baculoviruses (Nagamine et al., 2008) and parvoviruses (Ihalainen et al., 2009). While the molecular basis of host chromatin condensation and marginalization upon viral infection is unknown, it has been proposed to result from self-assembly when the maturing RCs and chromatin form two distinct compartments with high concentrations of incompatible components (Monier et al., 2000), from phase separation (Monier et al., 2000), or from depletion attraction (Ihalainen et al., 2009). In non-infected cells, chromatin condensation occurs in mitosis and apoptosis. Notably, a recent proteomics study reported an increase in histone PTM H3S10ph level upon lytic HSV-1 infection (Kulej et al., 2017). As this histone PTM is enriched in mitotic chromatin (Hendzel et al., 1997), it is interesting to speculate if virally induced chromatin condensation utilizes a naturally occurring mechanism.

Redistribution of host cell chromatin upon lytic HSV-1 infection is connected to viral RCs, which serve as the sites of viral genome replication and nucleocapsid assembly. Here, we studied the relative localization of host chromatin and viral RC marker protein ICP8 as a two-hour interval time point series between 12 and 24 h p.i. RCs originate as viral pre-replicative sites that can be observed within three hours p.i. (Burkham et al., 1998). Pre-replicative sites then expand and coalesce into mature RCs (Taylor et al., 2003). At 12 h p.i., most infected HeLa nuclei contained RCs that were in the process of merging. Host chromatin was condensed between adjacent RCs and to the nuclear periphery. At 16 h p.i., the RC regions appeared to reach the nuclear periphery at the sites of low-intensity DAPI stain. This was in concert with the previous observation of HEp-2 cell nuclei, in which a thin, intact layer of marginalized chromatin has been observed at 12 h p.i., followed by the breaching of the chromatin layer at 16 h p.i. as the RCs extend to the nuclear periphery (Simpson-Holley et al., 2005). Additionally, viral RC expansion and host chromatin marginalization in HeLa nuclei did not seem to progress further after 16–18 h p.i., which might therefore be the optimal time point for late infection studies with relatively intact nuclei.

HSV-1 RCs displace the surrounding host chromatin, which eventually condenses around the expanding RCs. Progeny HSV-1 nucleocapsids sized 125 nm in diameter are assembled in the nucleus, and must subsequently reach the inner nuclear membrane for nuclear egress. In addition to the chromatin breaches visible by light microscopy, soft X-ray tomography analysis has revealed separate channel-like structures spanning the condensed chromatin in mouse B lymphoblastoids at 24 hours p.i. (Myllys et al., 2016). These breaches and channels are thought to act as pathways through which progeny nucleocapsids are able to reach the nuclear periphery. In TEM micrographs, progeny nucleocapsids frequently accessed the nuclear envelope at gap sites, which contained sparse chromatin. Narrow egress channels spanning the marginalized chromatin revealed by soft X-ray tomography (Myllys et al., 2016) were undetectable due to the resolution limit of light microscopy, and were not unambiguously present in the thin slice sample set imaged on TEM for this study. However, as nucleocapsids seemed to repel the surrounding host chromatin from their imminent vicinity, it may be possible that multiple adjacent nucleocapsids could form transient channel-like structures, which might span even condensed host chromatin.

Controversial results have suggested HSV-1 nucleocapsid motility to be directed and actin-dependent (Forest et al., 2005), actin-independent (Bosse et al., 2014), and passive diffusion (Bosse et al., 2015). According to the model proposed by Bosse et al. (2015), nucleocapsids initially diffuse within and hop between interchromatin corrals, which enlarge upon HSV-1 infection. Expanding RCs, which might exclude nucleocapsids, eventually concentrate nucleocapsids close to the nuclear periphery, minimizing the distance nucleocapsids have to diffuse. The increased volume of corrals, and the extra membrane area of the flat-shaped, expanded nucleus enhance the diffusion strategy as the corrals next to the nuclear envelope are calculated to account for ~66% of the nuclear volume in infected cells (Bosse et al., 2015). Unfortunately, we were unable to detect well-defined chromatin corrals in this study. It is possible that a high-intensity chromatin stain combined with 3D imaging methods would be needed for the observation of corrals. However, intranuclear nucleocapsid distribution in our TEM and confocal imaging data did not fully support the speculation by Bosse et al., as no apparent exclusion of nucleocapsids from the central region of mature RCs could be seen,

although viral capsid protein VP26 did initially accumulate to the outer border region of RCs during live cell imaging. It would be tempting to approach the question of randomized nucleocapsid locations with statistical methods.

Finally, we studied the distribution of euchromatin and heterochromatin upon late HSV-1 infection by immunolabeling their respective histone PTMs. Although the HSV-1 genome is chromatinized upon nuclear entry (Kristie, 2015), the histone PTM labels used in this study co-localized rather with DAPI-stained host DNA than with viral RC regions, and likely indicated the chromatinization state of the host. The distribution of all observed histone PTMs changed along with marginalizing host chromatin. Notably, the transcriptionally active euchromatin was seen to marginalize to the nuclear periphery. The nuclear periphery is normally occupied by a layer of inactive heterochromatin, which was additionally detectable in the infected samples. Immunolabeling of both chromatin subtypes in the same sample could probably reveal if the marginalized euchromatin is still surrounded by a layer of heterochromatin, or if the epigenetic state of the peripheral heterochromatin is partially switched to active upon HSV-1 infection.

Histone PTMs are a regulatory mechanism for gene expression, which responds to cellular signals. It is therefore not surprising that viral infection can induce alterations in histone PTMs. A recent study by Kulej et al. (2017) detected significant regulation in 53 histone PTMs upon HSV-1 infection, including downregulation of H3K4me3, and upregulation of H3K9ac. As both PTMs are associated with euchromatin, this phenomenon might originate from different subsets of genes, which are either shut off or switched on upon HSV-1 infection (Kulej et al., 2017). Although the euchromatin marker H3K27ac was not included in the proteomics study by Kujel et al., it is possible that the peripheral euchromatin observed in our study might represent virally induced chromatin activation. Since gene transcription is thought to require loosely packaged euchromatin, this could possibly be related to the large transcripts of normally silenced genes, which result from virally disrupted termination of host transcription (Rutkowski et al., 2015). Additionally, the physical properties of less condensed euchromatin might promote viral RC expansion and nucleocapsid movement towards the inner

nuclear membrane.

The surprising observation of intensity differences between DAPI-stained host chromatin and histone PTM labels might result from single-stranded DNA, as postulated by Dr. Mäntylä (University of Jyväskylä, personal communication). DAPI binds the minor groove of double-stranded DNA (reviewed by Chazotte, 2011), and is not considered useful in detecting short DNA fragments. However, nucleosome-like complexes have been shown to remain associated with single-stranded DNA (Palter et al., 1979; Adkins et al., 2017). Chromatin condensation during mitosis causes torsional stress, which can result in the formation of hairpin structures recognized by single-strand DNA nucleases (Juan et al., 1996). Furthermore, double-strand breaks are known to appear in mitotic DNA especially at specific loci called common fragile sites (reviewed by Gelot et al., 2015). HSV-1 infection disintegrates the nuclear lamina by a mechanism, which is likely to disrupt the interactions between lamin B receptor, heterochromatin binding proteins, and heterochromatin histone PTM H3K9me3 (Kulej et al., 2017). It is interesting to speculate if the untethered heterochromatin and condensed euchromatin are subjected to integrity loss as the viral RCs breach towards the inner nuclear envelope.

Technically, this study was complicated by asynchronous and secondary infections, which made the determination of true post infection time points difficult. Observation of the phases of infection, and comparison to the timing of events mentioned in literature, would benefit from the synchronized infection protocol described by Pomeranz and Blaho (1999). It is noteworthy, though, that an MOI of 30 was required to ensure synchronous infection of all Vero cells under the low-temperature adsorption conditions (Pomeranz and Blaho, 1999). Although the effective MOI was calculated to be 7 PFU/cell, the effects of the resulting high virus load should be tested for each cell line and virus strain prior to adopting the protocol.

6. Future perspectives

From a cell biology point of view, HSV-1 is associated with elegant replication strategies, which directly utilize the center of eukaryotic life – the nucleus. This study aimed to shed some light on the complex interactions between HSV-1 and the host cell nucleus, with a specific emphasis on the alterations in the host chromatin. Viral RCs occupy the nuclear interior during replication and nucleocapsid assembly. Host euchromatin is marginalized to the nuclear periphery, where it acts as a dense barrier in addition to the naturally occurring layer of peripheral heterochromatin. The mechanism by which HSV-1 induces host chromatin condensation remains elusive. It is likewise unknown how viral RC regions displace the dense host chromatin for the formation of gaps and channels that extend to the inner nuclear envelope. These questions could possibly be approached by further studies on the properties of host chromatin upon HSV-1 infection. Viruses generally take advantage of pre-existing cellular functions; it would therefore be interesting to compare the condensed chromatin in mitosis and apoptosis to the condensed chromatin in HSV-1 infection. The use of additional histone PTM markers could be considered since specific histone modifications, such as the acetylation state of histone H4K16, are known to be involved in chromatin condensation during mitosis (Shogren-Knaak et al., 2006; Wilkins et al., 2014)

As a human pathogen, HSV-1 causes a lifelong infection affecting an estimated 67% of the global population (Looker et al., 2015). Although the typical symptoms of sporadic HSV-1 reactivation episodes may be considered relatively mild, in rare cases HSV-1 infection can lead to blindness (reviewed by Toma et al., 2008) or severe encephalitis (reviewed by Levitz, 1998). Moreover, neonate HSV-1 infections have high mortality rates (Harris and Holmes, 2017). Antiviral drugs such as acyclovir have been shown to decrease lesion formation, and improve lesion healing times by approximately 10–15% during an active episode of HSV-1 infection (Harmenberg et al., 2010). Considering the high global HSV-1 incidence, modest effect of current antivirals, and the possibility of antiviral resistance (Kakiuchi et al., 2013; Frobert et al., 2014) there is a reasonable need for alternative and improved HSV-1 therapeutics. Profound understanding of the viral life cycle can reveal novel therapeutic targets

for treating or preventing an active HSV-1 infection.

7. References

Adkins, N.L., S.G. Swygert, P. Kaur, H. Niu, S.A. Grigoryev, P. Sung, H. Wang, and C.L. Peterson. 2017. Nucleosome-like, Single-stranded DNA (ssDNA)-Histone Octamer Complexes and the Implication for DNA Double Strand Break Repair. *J.Biol.Chem.* 292:5271-5281.

Aho, V., M. Myllys, V. Ruokolainen, S. Hakanen, E. Mantyla, J. Virtanen, V. Hukkanen, T. Kuhn, J. Timonen, K. Mattila, C.A. Larabell, and M. Vihinen-Ranta. 2017. Chromatin organization regulates viral egress dynamics. *Sci.Rep.* 7:3692-017-03630-y

Allfrey, V.G., R. Faulkner, and A.E. Mirsky. 1964. Acetylation and Methylation of Histones and their Possible Role in the Regulation of Rna Synthesis. *Proc.Natl.Acad.Sci.U.S.A.* 51:786-794.

Alwine, J.C., W.L. Steinhart, and C.W. Hill. 1974. Transcription of herpes simplex type 1 DNA in nuclei isolated from infected HEp-2 and KB cells. *Virology.* 60:302-307.

Annunziato, A. 2008. DNA Packaging: Nucleosomes and Chromatin. *Nature Education* 1(1):26

Bannister, A.J., and T. Kouzarides. 2011. Regulation of chromatin by histone modifications. *Cell Res.* 21:381-395.

Bigalke, J.M., and E.E. Heldwein. 2016. Nuclear Exodus: Herpesviruses Lead the Way. *Annu.Rev.Virol.* 3:387-409.

Bosse, J.B., I.B. Hogue, M. Feric, S.Y. Thiberge, B. Sodeik, C.P. Brangwynne, and L.W. Enquist. 2015. Remodeling nuclear architecture allows efficient transport of herpesvirus capsids by diffusion. *Proc.Natl.Acad.Sci.U.S.A.* 112:E5725-33.

Bosse, J.B., S. Virding, S.Y. Thiberge, J. Scherer, H. Wodrich, Z. Ruzsics, U.H. Koszinowski, and L.W. Enquist. 2014. Nuclear herpesvirus capsid motility is not dependent on F-actin. *MBio.* 5:e01909-14.

Brown, J.C., and W.W. Newcomb. 2011. Herpesvirus capsid assembly: insights from structural analysis. *Curr.Opin.Virol.* 1:142-149.

Burkham, J., D.M. Coen, and S.K. Weller. 1998. ND10 protein PML is recruited to herpes simplex virus type 1 prereplicative sites and replication compartments in the presence of viral DNA polymerase. *J.Virol.* 72:10100-10107.

Chang, L., W.J. Godinez, I.H. Kim, M. Tektonidis, P. de Lanerolle, R. Eils, K. Rohr, and D.M. Knipe. 2011. Herpesviral replication compartments move and coalesce at nuclear speckles to enhance export of viral late mRNA. *Proc.Natl.Acad.Sci.U.S.A.* 108:E136-44.

Chazotte, B. 2011. Labeling nuclear DNA using DAPI. *Cold Spring Harb Protoc.* 2011:pdb.prot5556.

Davies, H.G., and J.V. Small. 1968. Structural units in chromatin and their orientation on membranes. *Nature.* 217:1122-1125.

Deshmane, S.L., and N.W. Fraser. 1989. During latency, herpes simplex virus type 1 DNA is associated with nucleosomes in a chromatin structure. *J.Virol.* 63:943-947.

Dix, R.D., R.R. McKendall, and J.R. Baringer. 1983. Comparative neurovirulence of herpes simplex virus type 1 strains after peripheral or intracerebral inoculation of BALB/c mice. *Infect.Immun.* 40:103-112.

Forest, T., S. Barnard, and J.D. Baines. 2005. Active intranuclear movement of herpesvirus capsids. *Nat.Cell Biol.* 7:429-431.

Frobert, E., S. Burrel, S. Ducastelle-Lepretre, G. Billaud, F. Ader, J.S. Casalegno, V. Nave, D. Boutolleau, M. Michallet, B. Lina, and F. Morfin. 2014. Resistance of herpes simplex viruses to acyclovir: an update from a ten-year survey in France. *Antiviral Res.* 111:36-41.

Gelot, C., I. Magdalou, and B.S. Lopez. 2015. Replication stress in Mammalian cells and its consequences for mitosis. *Genes (Basel).* 6:267-298.

Goldman, R.D., Y. Gruenbaum, R.D. Moir, D.K. Shumaker, and T.P. Spann. 2002. Nuclear lamins: building blocks of nuclear architecture. *Genes Dev.* 16:533-547.

Grunewald, K., P. Desai, D.C. Winkler, J.B. Heymann, D.M. Belnap, W. Baumeister, and A.C. Steven. 2003. Three-dimensional structure of herpes simplex virus from cryo-electron tomography. *Science.* 302:1396-1398.

Guo, H., S. Shen, L. Wang, and H. Deng. 2010. Role of tegument proteins in herpesvirus assembly and egress. *Protein Cell.* 1:987-998.

Harmenberg, J., B. Oberg, and S. Spruance. 2010. Prevention of ulcerative lesions by episodic treatment of recurrent herpes labialis: A literature review. *Acta Derm.Venereol.* 90:122-130.

Harris, J.B., and A.P. Holmes. 2017. Neonatal Herpes Simplex Viral Infections and Acyclovir: An Update. *J.Pediatr.Pharmacol.Ther.* 22:88-93.

Hayward, G.S., R.J. Jacob, S.C. Wadsworth, and B. Roizman. 1975. Anatomy of herpes simplex virus DNA: evidence for four populations of molecules that differ in the relative orientations of their long and short components. *Proc.Natl.Acad.Sci.U.S.A.* 72:4243-4247.

Hendzel, M.J., Y. Wei, M.A. Mancini, A. Van Hooser, T. Ranalli, B.R. Brinkley, D.P. Bazett-Jones, and C.D. Allis. 1997. Mitosis-specific phosphorylation of histone H3 initiates primarily within pericentromeric heterochromatin during G2 and spreads in an ordered fashion coincident with mitotic chromosome condensation. *Chromosoma.* 106:348-360.

Ihalainen, T.O., E.A. Niskanen, J. Jylhava, O. Paloheimo, N. Dross, H. Smolander, J. Langowski, J. Timonen, and M. Vihinen-Ranta. 2009. Parvovirus induced alterations in nuclear architecture and dynamics. *PLoS One.* 4:e5948.

Jacob, R.J., and B. Roizman. 1977. Anatomy of herpes simplex virus DNA VIII. Properties of the replicating DNA. *J.Virol.* 23:394-411.

Juan, G., W. Pan, and Z. Darzynkiewicz. 1996. DNA segments sensitive to single-strand-specific nucleases are present in chromatin of mitotic cells. *Exp.Cell Res.* 227:197-202.

Kakiuchi, S., S. Nonoyama, H. Wakamatsu, K. Kogawa, L. Wang, H. Kinoshita-Yamaguchi, M. Takayama-Ito, C.K. Lim, N. Inoue, M. Mizuguchi, T. Igarashi, and M. Saijo. 2013. Neonatal herpes encephalitis caused by a virologically confirmed acyclovir-resistant herpes simplex virus 1 strain. *J.Clin.Microbiol.* 51:356-359.

Kelly, B.J., C. Fraefel, A.L. Cunningham, and R.J. Diefenbach. 2009. Functional roles of the tegument proteins of herpes simplex virus type 1. *Virus Res.* 145:173-186.

Kent, J.R., P.Y. Zeng, D. Atanasiu, J. Gardner, N.W. Fraser, and S.L. Berger. 2004. During lytic infection herpes simplex virus type 1 is associated with histones bearing modifications that correlate with active transcription. *J.Virol.* 78:10178-10186.

Kristie, T.M. 2015. Dynamic modulation of HSV chromatin drives initiation of infection and provides targets for epigenetic therapies. *Virology.* 479-480:555-561.

Kukhanova, M.K., A.N. Korovina, and S.N. Kochetkov. 2014. Human herpes simplex virus: life cycle and development of inhibitors. *Biochemistry (Mosc).* 79:1635-1652.

Kulej, K., D.C. Avgousti, S. Sidoli, C. Herrmann, A.N. Della Fera, E.T. Kim, B.A. Garcia, and M.D. Weitzman. 2017. Time-resolved Global and Chromatin Proteomics during Herpes Simplex Virus Type 1 (HSV-1) Infection. *Mol.Cell.Proteomics.* 16:S92-S107.

Lamers, S.L., R.M. Newman, O. Laeyendecker, A.A. Tobian, R.C. Colgrove, S.C. Ray, D.M. Koelle, J. Cohen, D.M. Knipe, and T.C. Quinn. 2015. Global Diversity within and between Human Herpesvirus 1 and 2 Glycoproteins. *J.Virol.* 89:8206-8218.

Lehman, I.R., and P.E. Boehmer. 1999. Replication of herpes simplex virus DNA. *J.Biol.Chem.* 274:28059-28062.

Levitz, R.E. 1998. Herpes simplex encephalitis: a review. *Heart Lung.* 27:209-212.

Looker, K.J., A.S. Magaret, M.T. May, K.M. Turner, P. Vickerman, S.L. Gottlieb, and L.M. Newman. 2015. Global and Regional Estimates of Prevalent and Incident Herpes Simplex Virus Type 1 Infections in 2012. *PLoS One.* 10:e0140765.

Loret, S., G. Guay, and R. Lippe. 2008. Comprehensive characterization of extracellular herpes simplex virus type 1 virions. *J.Virol.* 82:8605-8618.

Luger, K., A.W. Mader, R.K. Richmond, D.F. Sargent, and T.J. Richmond. 1997. Crystal structure of the nucleosome core particle at 2.8 A resolution. *Nature.* 389:251-260.

Maul, G.G., H.H. Guldner, and J.G. Spivack. 1993. Modification of discrete nuclear domains induced by herpes simplex virus type 1 immediate early gene 1 product (ICP0). *J.Gen.Virol.* 74 (Pt 12):2679-2690.

McGeoch, D.J., F.J. Rixon, and A.J. Davison. 2006. Topics in herpesvirus genomics and evolution. *Virus Res.* 117:90-104.

McVoy, M.A., D.E. Nixon, J.K. Hur, and S.P. Adler. 2000. The ends on herpesvirus DNA replicative concatemers contain pac2 cis cleavage/packaging elements and their formation is controlled by terminal cis sequences. *J.Virol.* 74:1587-1592.

Monier, K., J.C. Armas, S. Etteldorf, P. Ghazal, and K.F. Sullivan. 2000. Annexation of the interchromosomal space during viral infection. *Nat.Cell Biol.* 2:661-665.

Myllys, M., V. Ruokolainen, V. Aho, E.A. Smith, S. Hakanen, P. Peri, A. Salvetti, J. Timonen, V. Hukkanen, C.A. Larabell, and M. Vihinen-Ranta. 2016. Herpes simplex virus 1 induces egress channels through marginalized host chromatin. *Sci.Rep.* 6:28844.

Nagamine, T., Y. Kawasaki, A. Abe, and S. Matsumoto. 2008. Nuclear marginalization of host cell chromatin associated with expansion of two discrete virus-induced subnuclear compartments during baculovirus infection. *J.Virol.* 82:6409-6418.

Newcomb, W.W., B.L. Trus, F.P. Booy, A.C. Steven, J.S. Wall, and J.C. Brown. 1993. Structure of the herpes simplex virus capsid. Molecular composition of the pentons and the triplexes. *J.Mol.Biol.* 232:499-511.

Nicoll, M.P., J.T. Proenca, V. Connor, and S. Efstathiou. 2012. Influence of herpes simplex virus 1 latency-associated transcripts on the establishment and maintenance of latency in the ROSA26R reporter mouse model. *J.Virol.* 86:8848-8858.

Palter, K.B., V.E. Foe, and B.M. Alberts. 1979. Evidence for the formation of nucleosome-like histone complexes on single-stranded DNA. *Cell.* 18:451-467.

Pante, N., and M. Kann. 2002. Nuclear pore complex is able to transport macromolecules with diameters of about 39 nm. *Mol.Biol.Cell.* 13:425-434.

Poffenberger, K.L., and B. Roizman. 1985. A noninverting genome of a viable herpes simplex virus 1: presence of head-to-tail linkages in packaged genomes and requirements for circularization after infection. *J.Virol.* 53:587-595

Pomeranz, L.E., and J.A. Blaho. 1999. Modified VP22 localizes to the cell nucleus during synchronized herpes simplex virus type 1 infection. *J.Virol.* 73:6769-6781.

Robinson, P.J., L. Fairall, V.A. Huynh, and D. Rhodes. 2006. EM measurements define the dimensions of the "30-nm" chromatin fiber: evidence for a compact, interdigitated structure. *Proc.Natl.Acad.Sci.U.S.A.* 103:6506-6511.

Rock, D.L., and N.W. Fraser. 1983. Detection of HSV-1 genome in central nervous system of latently infected mice. *Nature.* 302:523-525.

Rutkowski, A.J., F. Erhard, A. L'Hernault, T. Bonfert, M. Schilhabel, C. Crump, P. Rosenstiel, S. Efstathiou, R. Zimmer, C.C. Friedel, and L. Dolken. 2015. Widespread disruption of host transcription termination in HSV-1 infection. *Nat.Commun.* 6:7126.

Schwartz, J., and B. Roizman. 1969. Similarities and Differences in the Development of Laboratory Strains and Freshly Isolated Strains of Herpes Simplex Virus in HEp-2 Cells: Electron Microscopy. *J.Virol.* 4:879-889.

Shi, J., and R.K. Dawe. 2006. Partitioning of the maize epigenome by the number of methyl groups on histone H3 lysines 9 and 27. *Genetics.* 173:1571-1583.

Shogren-Knaak, M., H. Ishii, J.M. Sun, M.J. Pazin, J.R. Davie, and C.L. Peterson. 2006. Histone H4-K16 acetylation controls chromatin structure and protein interactions. *Science.* 311:844-847.

Simpson-Holley, M., J. Baines, R. Roller, and D.M. Knipe. 2004a. Herpes simplex virus 1 U(L)31 and U(L)34 gene products promote the late maturation of viral replication compartments to the nuclear periphery. *J.Virol.* 78:5591-5600.

Simpson-Holley, M., J. Baines, R. Roller, and D.M. Knipe. 2004b. Herpes simplex virus 1 U(L)31 and U(L)34 gene products promote the late maturation of viral replication compartments to the nuclear periphery. *J.Virol.* 78:5591-5600.

Simpson-Holley, M., R.C. Colgrove, G. Nalepa, J.W. Harper, and D.M. Knipe. 2005. Identification and functional evaluation of cellular and viral factors involved in the alteration of nuclear architecture during herpes simplex virus 1 infection. *J.Virol.* 79:12840-12851.

Skepper, J.N., A. Whiteley, H. Browne, and A. Minson. 2001. Herpes simplex virus nucleocapsids mature to progeny virions by an envelopment --> deenvelopment --> reenvelopment pathway. *J.Virol.* 75:5697-5702.

Strang, B.L., and N.D. Stow. 2005. Circularization of the herpes simplex virus type 1 genome upon lytic infection. *J.Virol.* 79:12487-12494.

Suka, N., Y. Suka, A.A. Carmen, J. Wu, and M. Grunstein. 2001. Highly specific antibodies determine histone acetylation site usage in yeast heterochromatin and euchromatin. *Mol.Cell.* 8:473-479.

Szpara, M.L., D. Gatherer, A. Ochoa, B. Greenbaum, A. Dolan, R.J. Bowden, L.W. Enquist, M. Legendre, and A.J. Davison. 2014. Evolution and diversity in human herpes simplex virus genomes. *J.Virol.* 88:1209-1227.

Taylor, T.J., E.E. McNamee, C. Day, and D.M. Knipe. 2003. Herpes simplex virus replication compartments can form by coalescence of smaller compartments. *Virology.* 309:232-247.

Tie, F., R. Banerjee, C.A. Stratton, J. Prasad-Sinha, V. Stepanik, A. Zlobin, M.O. Diaz, P.C. Scacheri, and P.J. Harte. 2009. CBP-mediated acetylation of histone H3 lysine 27 antagonizes Drosophila Polycomb silencing. *Development.* 136:3131-3141.

Toma, H.S., A.T. Murina, R.G. Areaux Jr, D.M. Neumann, P.S. Bhattacharjee, T.P. Foster, H.E. Kaufman, and J.M. Hill. 2008. Ocular HSV-1 latency, reactivation and recurrent disease. *Semin.Ophthalmol.* 23:249-273.

Venkatesh, S., and J.L. Workman. 2015. Histone exchange, chromatin structure and the regulation of transcription. *Nat.Rev.Mol.Cell Biol.* 16:178-189.

Wang, H., D.J. Davido, and L.A. Morrison. 2013. HSV-1 strain McKrae is more neuroinvasive than HSV-1 KOS after corneal or vaginal inoculation in mice. *Virus Res.* 173:436-440.

Whitley, R., D.W. Kimberlin, and C.G. Prober. 2007. Pathogenesis and disease. *In* Human Herpesviruses: Biology, Therapy, and Immunoprophylaxis. A. Arvin, G. Campadelli-Fiume, E. Mocarski, P.S. Moore, B. Roizman, R. Whitley and K. Yamanishi, editors. , Cambridge.

Wilkins, B.J., N.A. Rall, Y. Ostwal, T. Kruitwagen, K. Hiragami-Hamada, M. Winkler, Y. Barral, W. Fischle, and H. Neumann. 2014. A cascade of histone modifications induces chromatin condensation in mitosis. *Science.* 343:77-80.

Zhou, Z.H., M. Dougherty, J. Jakana, J. He, F.J. Rixon, and W. Chiu. 2000. Seeing the herpesvirus capsid at 8.5 A. *Science.* 288:877-880.

Zimber, A., Q.D. Nguyen, and C. Gespach. 2004. Nuclear bodies and compartments: functional roles and cellular signalling in health and disease. *Cell.Signal.* 16:1085-1104.